Novel Quaternary Lanthanum Bismuth Sulfides $Pb_2La_xBi_{8-x}S_{14}$, $Sr_2La_xBi_{8-x}S_{14}$, and $Cs_2La_xBi_{10-x}S_{16}$ with Complex Structures

Lykourgos Iordanidis and Mercouri G. Kanatzidis*

Department of Chemistry and Center for Fundamental Materials Research, Michigan State University, East Lansing, Michigan 48824

Received October 18, 2000

The compounds $Pb_2La_xBi_{8-x}S_{14}$ (**I**), $Sr_2La_xBi_{8-x}S_{14}$ (**II**), and $Cs_2La_xBi_{10-x}S_{16}$ (**III**) were synthesized from the corresponding elements or binary sulfides at temperatures above 850 °C. Compounds **I** and **II** are isostructural, forming a new structure type, while the structure of **III** is related to the structure of the mineral kobellite. All compounds crystallize in the orthorhombic space group *Pnma* (No. 62) with $a = 21.2592(4)$ Å, $b = 4.0418(1)$ Å, $c = 28.1718(3)$ Å, $Z = 4$ for **I**, $a = 21.190(1)$ Å, $b = 4.0417(2)$ Å, $c = 28.285(2)$ Å, $Z = 4$ for **II** and $a = 34.893(4)$ Å, $b = 4.0697(4)$ Å, $c = 21.508(2)$ Å, $Z = 4$ for **III**. All compounds exhibit mixed site occupancy between Bi and La. Furthermore, **I** and **II** exhibit disorder between the divalent atom (Sr or Pb) and/or La and/or Bi. The structures of **I** and **II** consist of thin walls made of two metal-atom-thick NaCl-type blocks running in two opposite directions in the *ac* plane, forming rhombus-shaped tunnels. These tunnels are filled with Bi_2Te_3-type fragments. In the points where the walls intersect they form Gd_2S_3-type fragments. The structure of **III** consists of a complex three-dimensional framework with Cs-filled tunnels. All compounds are semiconductors with band gaps around 1.0 eV, and they melt around 740−860 °C.

Introduction

Synthetic investigations in multinary bismuth chalcogenides systems in the past decade have contributed a great number of new compounds such as β-,γ-$CsBiS_2$,[1] KBi_3S_5,[2] $KBi_{6.33}S_{10}$,[3] $K_2Bi_8S_{13}$,[3] α-,β-$K_2Bi_8Se_{13}$,[1,4] $K_{2.5}Bi_{8.5}Se_{14}$,[4] $A_xBi_4Se_7$[5] ($x = 1, 2$; A = Rb, Cs), $Cs_xBi_7Se_{12}$[5] ($x = 1$, 2, or 3), ABi_3Q_5[6] (A = Rb, Cs; Q = S, Se, Te), $A_2Bi_8Se_{13}$[7] (A = Rb, Cs), $CsBi_{3.67}Se_6$,[7] $BaBi_2Se_4$,[7] $Ba_3Bi_{6.67}Se_{13}$,[8] $BaBiTe_3$,[9] $CsBi_4Te_6$,[10] $Sn_4Bi_2Se_7$,[11] $SnBi_4Se_7$,[12] $CdBi_2S_4$,[13] $CdBi_4S_7$,[13] $Cd_{2.8}Bi_{8.1}S_{15}$,[13] $Cd_2Bi_6S_{11}$,[13] $APbBi_3Se_6$[14] (A = K, Rb, Cs), $K_{1-x}Sn_{5-x}Bi_{11+x}Se_{22}$,[15] $A_{1+x}M'_{4-2x}Bi_{7+x}Se_{15}$[16] (A = K, Rb; M′ = Sn, Pb), and $Ba_3MBi_6Se_{13}$[8] (M = Sn, Pb). The great majority of these phases, often not found in the corresponding published phase diagrams, feature novel structure types reminiscent of, but distinct from, those of the mineral sulfosalts. Small changes in the synthetic conditions and elemental ratio can result in new phases, in contrast to many other multinary systems that tend to give mixtures of known phases. The rich compositional and structural variety makes them some of the most adaptable and versatile systems in solid-state chemistry.

In addition, bismuth atoms both in the compounds mentioned above and in the natural sulfosalts exhibit an astonishing bonding flexibility, occupying sites with coordination numbers from 6 (octahedral, most of the times distorted) up to 9.[1−17] These sites with coordination number greater than 6 connect with one another the several NaCl-, Bi_2Te_3-, CdI_2-, and Sb_2Se_3-type blocks, formed by the BiQ_6 (Q = chalcogen) octahedra when combined together by sharing edges. Often bismuth atoms participate in mixed site occupation with similarly sized atoms, e.g., Pb, Sn, lanthanide, alkali metal, or alkaline earth metal atoms. Because of the size similarity of Bi^{3+} to several Ln^{3+}

(1) McCarthy, T. J.; Ngeyi, S.-P.; Liao, J.-H.; DeGroot, D. C.; Hogan, T.; Kannewurf, C. R.; Kanatzidis, M. G. *Chem. Mater.* **1993**, *5*, 331−340.
(2) McCarthy, T. J.; Tanzer, T. A.; Kanatzidis, M. G. *J. Am. Chem. Soc.* **1995**, *117*, 1294−1301.
(3) (a) Kanatzidis, M. G.; McCarthy, T. J.; Tanzer, T. A.; Chen, L.-H.; Iordanidis, L.; Hogan, T.; Kannewurf, C. R.; Uher, C.; Chen, B. *Chem. Mater.* **1996**, *8*, 1465−1474. (b) Chen, B.; Uher, C.; Iordanidis, L.; Kanatzidis, M. G. *Chem. Mater.* **1997**, *9*, 1655−1658.
(4) Chung, D.-Y.; Choi, K.-S.; Iordanidis, L.; Schindler, J. L.; Brazis, P. W.; Kannewurf, C. R.; Chen, B.; Hu, S.; Uher, C.; Kanatzidis, M. G. *Chem. Mater.* **1997**, *9*, 3060−3071.
(5) (a) Iordanidis, L.; Kanatzidis, M. G. *Angew. Chem., Int. Ed.* **2000**, *39*, 1928−1930. (b) Iordanidis, L.; Kanatzidis, M. G. *J. Am. Chem. Soc.* **2000**, *122*, 8319−8320.
(6) Iordanidis, L.; Kanatzidis, M. G. Manuscript in preparation.
(7) Iordanidis, L.; Brazis, P. W.; Kyratsi, T.; Ireland, J.; Lane, M.; Kannewurf, C. R.; Dyck, J. S.; Uher, C.; Ghelani, N. A.; Hogan, T.; Kanatzidis, M. G. *Chem. Mater.* **2001**, *13*, 622−633.
(8) Wang, Y. C.; DiSalvo, F. J. *Chem. Mater.* **2000**, *12*, 1011−1017.
(9) Chung, D.-Y.; Jobic, S.; Hogan, T.; Kannewurf, C. R.; Brec, R.; Rouxel, R.; Kanatzidis, M. G. *J. Am. Chem. Soc.* **1997**, *119*, 2505−2515.
(10) Chung, D.-Y.; Hogan, T.; Brazis, P.; Rocci-Lane, M.; Kannewurf, C.; Bastea, M.; Uher, C.; Kanatzidis, M. G. *Science* **2000**, *287*, 1024−1027.
(11) Adouby, K.; Perez Vicente, C.; Jumas, J. C.; Fourcade, R.; Abba Touré, A. *Z. Kristallogr.* **1998**, *213*, 343−349.
(12) Perez Vicente, C.; Tirado, J. L.; Adouby, K.; Jumas, J. C.; Abba Touré, A.; Kra, G. *Inorg. Chem.* **1999**, *38*, 2131−2135.
(13) Choe, W.; Lee, S.; O'Connell, P.; Covey, A. *Chem. Mater.* **1997**, *9*, 2025−2030.
(14) Chung, D.-Y.; Iordanidis, L.; Rangan, K. K.; Brazis, P. W.; Kannewurf, C. R.; Kanatzidis, M. G. *Chem. Mater.* **1999**, *11*, 1352−1362.
(15) Mrotzek, A.; Chung, D.-Y.; Hogan, T.; Kanatzidis, M. G. *J. Mater. Chem.* **2000**, *10*, 1667−1672.
(16) Choi, K.-S.; Chung, D.-Y.; Mrotzek, A.; Brazis, P. W.; Kannewurf, C. R.; Kanatzidis, M. G. *Chem. Mater.*, in press.
(17) (a) Iitaka, Y.; Nowacki, W. *Acta Crystallogr.* **1962**, *15*, 691−698. (b) Takeuchi, Y.; Takagi, J. *Proc. Jpn. Acad.* **1974**, *50*, 222−225. (c) Takeuchi, Y.; Takagi, J.; Yamanaka, T. *Proc. Jpn. Acad.* **1974**, *50*, 317−321. (d) Takeuchi, Y.; Ozawa, T.; Takagi, J. *Z. Kristallogr.* **1979**, *150*, 75−84. (e) Otto, H. H.; Strunz, H. *Neues Jahrb. Mineral., Abh.* **1968**, *108*, 1−19. (f) Srikrishnan, T.; Nowacki, W. *Z. Kristallogr., Kristallgeom., Kristallphys., Kristallchem.* **1974**, *140*, 114−136. (g) Tilley, R. J. D.; Wright, A. C. *J. Solid State Chem.* **1986**, *65*, 45−62. (h) Takagi, J.; Takeuchi, Y. *Acta Crystallogr., Sect. B* **1972**, *28*, 649−651. (i) Matzat, E. *Acta Crystallogr., Sect. B* **1979**, *35*, 133−136. (j) Takeuchi, Y.; Takagi, J. *Proc. Jpn. Acad.* **1974**, *50*, 76−79.

10.1021/ic001157v CCC: $20.00
Published on Web 03/10/2001

ions, possible mixed site occupation of Bi^{3+} and Ln^{3+} could enable the formation of novel structural types.

Furthermore, lanthanide−bismuth chalcogenide systems are relatively unexplored. Only a limited number is known, e.g., $EuBi_2S_4$,[18] Eu_2BiS_4,[19] $La_4Bi_2S_9$,[20] $Ce_{1.25}Bi_{3.78}S_8$,[21] $Eu_3Bi_4Q_9$ (Q = S, Se),[22] and they are little studied. Even less is known about quaternary lanthanide bismuth chalcogenides. For these reasons we decided to explore the solid-state chemistry of the A−Ln−Bi−Q systems (A = alkali or alkaline earth metal, M = lanthanide metal, Q = S, Se). We have already reported on $ALn_{1\pm x}Bi_{4\pm x}S_8$[23] (A = K, Rb; Ln = La, Ce, Pr, Nd) and $BaLaBi_2Q_6$[24] (Q = S, Se). We describe here the syntheses, physicochemical and spectroscopic characterization, and novel structures types of $Pb_2La_xBi_{8-x}S_{14}$, $Sr_2La_xBi_{8-x}S_{14}$, and $Cs_2La_xBi_{10-x}S_{16}$ and examine their relationships with other previously reported compounds.

Experimental Section

Reagents. Chemicals in this work were used as obtained: bismuth powder (99.999+%, −100 mesh, Cerac, Milwaukee, WI), bismuth chunks (99.999% Noranda, Canada), lead granules (99.999%, −20 mesh, Cerac, Milwaukee, WI), cesium metal (99.98%, Cerac, Milwaukee, WI), sulfur powder (sublimed, Spectrum Chemical Mfg. Corp., Gardena, CA), strontium sulfide (99.9% purity, −200 mesh, Cerac, Milwaukee, WI), lanthanum sulfide (99.9% purity, −200 mesh, Cerac, Milwaukee, WI). Cs_2S was prepared by a stoichiometric reaction of the cesium metal and sulfur in liquid ammonia as described earlier.[1]

Synthesis. All manipulations were carried out under a dry nitrogen atmosphere in a Vacuum Atmospheres Dri-Lab glovebox. All products were washed with degassed water, methanol, and ether to remove traces of excess flux. For all compounds the yield was almost quantitative, and the purity and homogeneity of the samples were verified by comparing the X-ray powder diffraction patterns to those calculated from the crystallographically determined fractional atomic coordinates.

1. Bi_2S_3. A mixture of 11.633 g (0.056 mol) of Bi and 2.677 g (0.083 mol) of S was transferred into a silica tube, which was flame-sealed under vacuum. The tube was heated to 650 °C in 48 h, kept at 650 °C for 2 days, and then cooled to 50 °C in 10 h. The product was ground into powder and used for further reactions.

2. $Pb_2La_xBi_{8-x}S_{14}$ (I). A mixture of 0.078 g (0.376 mmol) of Pb, 0.234 g (1.120 mmol) of Bi , 0.066 g (2.058 mmol) of S, and 0.140 g (0.374 mmol) of La_2S_3 was transferred to a carbon-coated silica tube that was flame-sealed under vacuum. The tube was heated for 99 h at 950 °C and was cooled to 550 °C at 10 °C/h and then to 50 °C in 10 h. The product consisted of long silver-gray needles. Scanning electron microscopy/energy-dispersive spectrometry (SEM/EDS) on a number of needles gave an average composition of $Pb_{2.3}La_{2.0}Bi_{6.3}S_{14}$.

3. $Sr_2La_xBi_{8-x}S_{14}$ (II). A mixture of 0.090 g (0.752 mmol) of SrS, 0.281 g (0.751 mmol) of La_2S_3, and 0.580 g (1.128 mmol) of Bi_2S_3 was transferred to a carbon-coated silica tube that was flame-sealed under vacuum. The tube was heated for 1 day at 950 °C and was cooled to 650 °C in 1 day and then to 50 °C in 11 h. The product consisted of long silver-gray needles. SEM/EDS on a number of needles gave an average composition of $Sr_{1.9}La_{2.2}Bi_{6.1}S_{15.6}$.

4. $Cs_2La_xBi_{10-x}S_{16}$ (III). A mixture of 0.040 g (0.134 mmol) of Cs_2S, 0.050 g (0.134 mmol) of La_2S_3, and 0.276 g (0.536 mmol) of Bi_2S_3 was transferred to a carbon-coated silica tube that was flame-sealed under vacuum. The tube was heated for 6 days at 900 °C and was cooled to 400 °C in 75 h and then to 50 °C in 10 h. The product consisted of long silver-gray needles. SEM/EDS on a number of needles gave an average composition of $Cs_{2.3}La_{1.1}Bi_{7.8}S_{16}$.

Physical Measurements. 1. Electron Microscopy. Quantitative microprobe analyses of the compounds were performed with a JEOL JSM-6400V scanning electron microscope equipped with either a Noran TN-5500 or a Noran Vantage energy dispersive spectroscopy detector. Data were collected for 45 s using an accelerating voltage of 25 kV. All reported results are an average of measurements on at least four different crystals.

2. Differential Thermal Analysis. Differential thermal analysis (DTA) was performed with a computer-controlled Shimadzu DTA-50 thermal analyzer. The ground single crystals (∼20 mg total mass) were sealed in carbon-coated silica ampules under vacuum. A silica ampule containing alumina of equal mass was sealed and placed on the reference side of the detector. The samples were heated to the desired temperature at 10 °C/min, then isothermed for 5 min followed by cooling at 10 °C/min to 150 °C and finally by rapid cooling to room temperature. The whole procedure was repeated to check for reproducibility. The reported DTA temperature is the peak temperature. The DTA samples were examined by using powder X-ray diffraction after the experiment.

3. Solid-State UV/Vis Spectroscopy. Optical diffuse reflectance measurements were made at room temperature with a Shimadzu UV-3101 PC double-beam double-monochromator spectrophotometer operating in the 200−2500 nm region. The instrument was equipped with an integrating sphere and controlled by a personal computer. $BaSO_4$ powder was used as reference (100% reflectance). The band gap was determined from the spectra as described elsewhere.[1]

4. Powder X-ray Diffraction. The compounds were examined by using X-ray powder diffraction to check for phase purity and for identification. Powder patterns were obtained using a Rigaku-Denki/Rw400F2 (Rotaflex) rotating-anode powder diffractometer or a CPS 120 INEL X-ray powder diffractometer equipped with a position-sensitive detector. The purity and homogeneity of all phases were confirmed by comparison of X-ray powder diffraction to those calculated from single-crystal data using the CERIUS[2] software.[25]

Single-Crystal X-ray Crystallography. A Bruker (formerly Siemens) SMART Platform CCD diffractometer was used for data collection. Several different sets of frames covering a random area of the reciprocal space were collected using 0.3° steps in ω at a detector-to-sample distance between 4 and 5 cm, depending on the desired resolution. The SMART software was used for data acquisition, and SAINT[26] was used for data extraction. The absorption correction was done with SADABS[26] and the structure solution (direct methods) and refinement was done with the SHELXTL[26] package of crystallographic programs. An analytical absorption correction was applied before SABABS for **II**.

1. $Pb_2La_xBi_{8-x}S_{14}$ (I). A hemisphere of data were collected (1271 frames) with an exposure time of 35 s per frame to a resolution of 0.75 Å. The final cell was calculated from 5289 [$I > 10\,\sigma(I)$] reflections chosen from the data set (Table 1). Ten metal atoms *Ml* and 14 sulfurs atoms were located on a crystallographic mirror plane, and the structure has the general formula $(Ml)_{10}S_{14}$ where *Ml* is any combination of Bi, Pb, or La. Initially all 10 metal positions were assigned and refined as Bi (R1 = 9.7%, wR2 = 20.6%). Pb and Bi, because of their chemical resemblance to each other and similar X-ray scattering properties, cannot be crystallographically distinguished. Furthermore, we know from previous results[23] and from $Cs_2La_xBi_{10-x}S_{16}$ (see below) that Bi and La atoms tend to adopt similar coordination environments and present mixed occupancy. In a subsequent step the occupancy of the 10 "bismuth" atoms was refined (R1 = 8.8%, wR2 = 17.5%). For four sites with octahedral coordination the occupancy did not change, while

(18) Lemoine, P.; Carre, D.; Guittard, M. *Acta Crystallogr., Sect. C* **1986**, *42*, 259−261.
(19) Lemoine, P.; Carre, D.; Guittard, M. *Acta Crystallogr., Sect. B* **1982**, *38*, 727−729.
(20) Ecrepont, C.; Guittard, M.; Flahaut, J. *Mater. Res. Bull.* **1988**, *23*, 37−42.
(21) Ceolin, R.; Toffoli, P.; Khodadad, P.; Rodier, N. *Acta Crystallogr., Sect. B* **1977**, *33*, 2804−2806.
(22) Aliev, O. M.; Maksudova, T. F.; Samsonova, N. D.; Finkel'shtein, L. D.; Rustamov, P. G. *Inorg. Mater.* **1986**, *22*, 23−27.
(23) Iordanidis, L.; Schindler, J. L.; Kannewurf, C. R.; Kanatzidis, M. G. *J. Solid State Chem.* **1999**, *143*, 151−162.
(24) Choi, K.-S.; Iordanidis, L.; Chondroudis, K.; Kanatzidis, M. G. *Inorg. Chem.* **1997**, *36*, 3804−3805.
(25) *CERIUS*^{2}, version 3.5; Molecular Simulations, Inc.: Cambridge, England, 1999.
(26) *SMART*, versions 4 and 5 (1996−1999); *SAINT*, versions 4, 5, and 6 (1994−1999); *SADABS*, *SHELXTL*, version 5.1; Bruker Analytical X-ray Systems, Inc.: Madison, WI.

Table 1. Crystallographic Data for $M_2La_xBi_{8-x}S_{14}$ (M = Pb, Sr) and $Cs_2La_xBi_{10-x}S_{16}$

	I	II	III
chemical formula	$Pb_2La_{2.10(6)}Bi_{5.90(6)}S_{14}$	$Sr_{2.00(5)}La_{2.58(5)}Bi_{5.42(3)}S_{14}$	$Cs_2La_{1.19(4)}Bi_{8.81(4)}S_{16}$
fw	2388.26	2113.23	2785.55
temp, K	296(2)	298(2)	296(2)
wavelength, Å (Mo Kα)	0.710 73	0.710 73	0.710 73
space group	*Pnma* (No. 62)	*Pnma* (No. 62)	*Pnma* (No. 62)
a, Å	21.2592(4)	21.190(1)	34.893(4)
b, Å	4.0418(1)	4.0417(2)	4.0697(4)
c, Å	28.1718(3)	28.285(2)	21.508(2)
Z, vol, Å^3	4, 2420.67(8)	4, 2422.4(2)	4, 3054.2(6)
density (calcd), g/cm^3	6.553	5.794	6.058
abs coeff, mm^{-1}	61.417	49.208	55.648
final *R* indices[a] [$I > 2\sigma(I)$]	R1 = 0.0465, wR2 = 0.0785	R1 = 0.0334, wR2 = 0.0633	R1 = 0.0497, wR2 = 0.0664
R indices[a] (all data)	R1 = 0.0786, wR2 = 0.0864	R1 = 0.0456, wR2 = 0.0668	R1 = 0.1226, wR2 = 0.0782

[a] $R1 = \sum||F_o| - |F_c||/\sum|F_o|$, $wR2 = \{\sum[w(F_o^2 - F_c^2)^2]/\sum[w(F_o^2)^2]\}^{1/2}$.

Table 2. Atomic Coordinates and Equivalent Isotropic Displacement Parameters (Å^2 × 10^3) for $Pb_2La_xBi_{8-x}S_{14}$[a]

cation site		*x*	*y*	*z*	*U*(eq)	occ
1	Bi(1)[b]	−0.4416(1)	−0.7500	0.4443(1)	18(1)	1
2	Bi(2)	−0.6432(1)	−0.7500	0.4414(1)	14(1)	1
3	Bi(3)	−0.3090(1)	−0.7500	0.3059(1)	17(1)	1
4	Bi(4)	0.0637(1)	0.2500	0.3020(1)	15(1)	1
5	M(5)	−0.0556(1)	−0.2500	0.4457(1)	18(1)	0.898(10)
	La(5)	−0.0556(1)	−0.2500	0.4457(1)	18(1)	0.102(10)
6	M(6)	0.1376(1)	−0.2500	0.4294(1)	24(1)	0.578(10)
	La(6)	0.1376(1)	−0.2500	0.4294(1)	24(1)	0.422(10)
7	M(7)	0.2611(1)	−0.2500	0.3226(1)	25(1)	0.469(10)
	La(7)	0.2611(1)	−0.2500	0.3226(1)	25(1)	0.531(10)
8	M(8)	−0.0330(1)	−0.2500	0.1680(1)	33(1)	0.691(11)
	La(8)	−0.0330(1)	−0.2500	0.1680(1)	33(1)	0.309(11)
9	M(9)	−0.2337(1)	−0.7500	0.4349(1)	36(1)	0.772(11)
	La(9)	−0.2337(1)	−0.7500	0.4349(1)	36(1)	0.228(11)
10	M(10)	−0.1243(1)	−0.2500	0.3097(1)	30(1)	0.496(10)
	La(10)	−0.1243(1)	−0.2500	0.3097(1)	30(1)	0.504(10)
	S(1)	−0.3528(2)	−0.2500	0.4523(2)	21(1)	
	S(2)	−0.4423(2)	−0.7500	0.3525(2)	17(1)	
	S(3)	−0.5397(2)	−0.2500	0.4386(2)	19(1)	
	S(4)	0.2746(2)	−0.2500	0.4376(2)	26(1)	
	S(5)	−0.6358(2)	−0.7500	0.3475(2)	16(1)	
	S(6)	−0.0445(2)	0.2500	0.2526(2)	19(1)	
	S(7)	−0.2059(2)	−0.7500	0.2565(2)	14(1)	
	S(8)	−0.2454(2)	−0.2500	0.3593(2)	15(1)	
	S(9)	0.1472(2)	−0.2500	0.2533(2)	20(1)	
	S(10)	0.1760(2)	0.2500	0.3629(2)	13(1)	
	S(11)	0.0209(2)	−0.2500	0.3550(2)	17(1)	
	S(12)	0.0369(2)	−0.7500	0.4562(2)	14(1)	
	S(13)	−0.1186(2)	−0.7500	0.3877(2)	13(1)	
	S(14)	0.1741(2)	−0.7500	0.5107(2)	16(1)	

[a] The positions with M(number) are occupied by Bi, Pb, or both. The number next to the metal atoms indicates the sites they belong in; e.g., La(5) and M(5) all belong to cation site 5. *U*(eq) is defined as one-third of the trace of the orthogonalized U_{ij} tensor. [b] See ref 30.

Table 3. Atomic Coordinates and Equivalent Isotropic Displacement Parameters (Å^2 × 10^3) for $Sr_2La_xBi_{8-x}S_{14}$[a]

cation site		*x*	*y*	*z*	*U*(eq)	occ
1	Bi(1)[§]	−0.4427(1)	−0.7500	0.4438(1)	18(1)	1
2	Bi(2)	−0.6425(1)	−0.7500	0.4402(1)	14(1)	1
3	Bi(3)	−0.3083(1)	−0.7500	0.3054(1)	16(1)	1
4	Bi(4)	0.0661(1)	0.2500	0.3033(1)	14(1)	1
A	Bi(5)	−0.0579(1)	−0.2500	0.4444(1)	17(1)	0.683(5)
5 A	Sr(5)	−0.0579(1)	−0.2500	0.4444(1)	17(1)	0.234(5)
B	Bi(5′)	−0.0663(4)	−0.132(3)	0.4566(3)	18(2)	0.042(2)
A	La(6)	0.1364(1)	−0.2500	0.4320(1)	12(1)	0.674(9)
6 A	Sr(6)	0.1364(1)	−0.2500	0.4320(1)	12(1)	0.293(8)
B	Bi(6)	0.1240(9)	−0.2500	0.4167(9)	27(5)	0.033(4)
7	La(7)	0.2624(1)	−0.2500	0.3220(1)	13(1)	0.556(7)
	Sr(7)	0.2624(1)	−0.2500	0.3220(1)	13(1)	0.444(7)
A	La(8)	−0.0311(1)	−0.2500	0.1717(1)	17(1)	0.538(14)
8 A	Sr(8)	−0.0311(1)	−0.2500	0.1717(1)	17(1)	0.325(10)
B	Bi(8)	−0.0283(2)	−0.2500	0.1581(3)	19(1)	0.137(6)
A	La(9)	−0.2469(1)	−0.7500	0.4405(1)	13(1)	0.407(10)
9 A	Sr(9)	−0.2469(1)	−0.7500	0.4405(1)	13(1)	0.188(8)
B	Bi(9)	−0.2293(1)	−0.7500	0.4291(1)	25(1)	0.404(4)
A	La(10)	−0.1194(1)	−0.2500	0.3088(1)	12(1)	0.401(10)
10 A	Sr(10)	−0.1194(1)	−0.2500	0.3088(1)	12(1)	0.516(9)
B	Bi(10)	−0.1401(5)	−0.2500	0.3160(3)	27(2)	0.083(4)
	S(1)	−0.3519(1)	−0.2500	0.4548(1)	18(1)	
	S(2)	−0.4387(1)	−0.7500	0.3536(1)	17(1)	
	S(3)	−0.5379(1)	−0.2500	0.4380(1)	18(1)	
	S(4)	0.2763(1)	−0.2500	0.4374(1)	25(1)	
	S(5)	−0.6349(1)	−0.7500	0.3467(1)	14(1)	
	S(6)	−0.0429(1)	0.2500	0.2529(1)	16(1)	
	S(7)	−0.2051(1)	−0.7500	0.2560(1)	14(1)	
	S(8)	−0.2463(1)	−0.2500	0.3600(1)	15(1)	
	S(9)	0.1466(1)	−0.2500	0.2530(1)	18(1)	
	S(10)	0.1771(1)	0.2500	0.3637(1)	11(1)	
	S(11)	0.0222(1)	0.2500	0.3554(1)	15(1)	
	S(12)	0.0387(1)	−0.7500	0.4559(1)	14(1)	
	S(13)	−0.1186(1)	−0.7500	0.3879(1)	14(1)	
	S(14)	0.1760(1)	−0.7500	0.5095(1)	17(1)	

[a] The number next to the metal atoms indicates the sites they belong in; e.g., La(8), Sr(8), and Bi(8) all belong to cation site 8. For the sites that exhibit splitting position A refers to the position in center of the site and position B to the position shifted away from the center to the side. *U*(eq) is defined as one-third of the trace of the orthogonalized U_{ij} tensor.

for the remaining six sites, with coordination numbers higher than 6 (7 or 8), the occupancy dropped to less than 0.5 (full theoretical occupancy). In these six sites, La was introduced in the refinement. The formula at that point was $La_{2.1}Bi_{7.9}S_{14}$; however, for charge-balancing purposes the compound should have the general formula $Pb_2(La,Bi)_8S_{14}$ or $Pb_2La_{2.1}Bi_{5.9}S_{14}$. This is agreement with the EDS/SEM data, which confirmed the presence of all four elements with $Pb_{2.3}La_{2.0}Bi_{6.3}S_{14}$ ratio. All atoms were refined anisotropically (R1 = 4.7%, wR2 = 7.9%). The fractional atomic coordinates and equivalent isotropic displacement parameters are shown in Table 2.

2. $Sr_2La_xBi_{8-x}S_{14}$ (II). Over a hemisphere of data were collected (1685 frames) with an exposure time of 45 s per frame to a resolution of 0.66 Å. The final cell was calculated from 10 670 [$I > 8\sigma(I)$] reflections (Table 1). Initially all 10 metal sites were assigned as Bi and their occupancies were refined (R1 = 9.8%, wR2 = 30.4%). Similar to what was found in the Pb compound above, the occupancies did not change in the four octahedral metal sites, indicating that they are occupied exclusively by Bi (sites 1−4) (Table 3). The occupancy of the remaining six sites (sites 5−10), with coordination numbers greater

than 6 (monocapped or bicapped trigonal prismatic), was refined to be less than 0.5 (theoretical full occupancy). One of the high coordinate sites, site 7, did not exhibit any splitting and was disordered between Sr and La only. A significant difference compared to **I** is that in **II** the remaining five of these six sites (sites 5, 6, 8−10) exhibit a splitting. In sites 6 and 8−10, one of the split atoms is sitting in the center of the site (A) and the other is shifted (∼0.4−0.5 Å) to the side (B) having a distorted octahedral or square pyramidal environment. That second position (B) was assigned as Bi, while the first (A) was disordered between La and Sr. The fifth highest coordinate site (site 5) also consists of two positions (A and B), but the splitting is different (see structure description). Initially both positions were refined as Bi and the total occupancy was 98%, suggesting that site 5 was mainly occupied by Bi. Attempts to change Bi in position B with lighter elements such as Sr or La resulted in over 100% total occupancy. The formula at that point with both positions A and B in site 5, assigned as Bi, was $Sr_{1.78}La_{2.58}Bi_{5.51}S_{14}$. Since there was less Sr in the structure than what is needed for charge neutrality, position B in site 5 was assigned as Bi (Bi5′) and position A in site 5 as Bi and Sr (Bi5/Sr5). The formula at that time was $Sr_{1.92}La_{2.51}Bi_{5.49}S_{14}$, very close to the ideal formula $Sr_2(La,Bi)_8S_{14}$. To verify this result, data were collected on three more crystals of $Sr_2La_xBi_{8-x}S_{14}$ from different synthetic batches, but the behavior of site 5 was identical. Individual constraints were used at each site to sum the total occupancy to 0.5000, and a general constraint was used to set the Sr amount to what was necessary for electroneutrality (R1 = 4.43%, wR2 = 8.90%). The four Bi atoms, La(7)/Sr(7), Bi(5)/Sr(5), and the 14 S atoms were refined anisotropically (R1 = 3.34%, wR2 = 6.33%). The final formula was $Sr_{2.00(5)}La_{2.58(5)}Bi_{5.42(3)}S_{14}$. The value of x varied between 2.4 and 2.7 in the other data sets. The fractional atomic coordinates and equivalent isotropic displacement parameters are shown in Table 3.

3. $Cs_2La_xBi_{10-x}S_{16}$ (III). A full sphere of data were collected (2082 frames) with an exposure time of 62 s per frame with 0.74 Å resolution. The final cell was calculated from 3553 [$I > 10\,\sigma(I)$] reflections (Table 1). Initially two cesium, 16 sulfur, and 10 "bismuth" atoms were found. After refinement the R values were R1 = 8.2% and wR2 = 14.1%. Three of the "bismuth" atoms with bicapped trigonal prismatic coordination had a relatively high isotropic displacement parameter, $U_{iso} \approx 0.050$ Å^2, compared to that of the other octahedral bismuth atoms, $U_{iso} \approx 0.015$ Å^2. A disorder model with La and Bi was used for these three sites (R1 = 7.7%, wR2 = 12.5%). All the atoms were refined anisotropically (R1 = 5.0%, wR2 = 6.6%). The final formula was $Cs_2La_{1.19(4)}Bi_{8.81(4)}S_{16}$. The fractional atomic coordinates and equivalent isotropic displacement parameters are shown in Table 4.

Results and Discussion

Synthesis, Thermal Analysis, and Spectroscopy. $Pb_2La_xBi_{8-x}S_{14}$ ($x \approx 2.1$) was synthesized by reacting Pb/Bi/La_2S_3/S in a 1:3:1:5.5 ratio at 950 °C. This phase seems to be the most stable in this system, and attempts to vary the amount of any of the reactants resulted in a mixture of **I** with the corresponding binary compounds. When a lower amount of La_2S_3 was used, Pb/Bi/S ternary phases were found. The same was also true for $Sr_2La_xBi_{8-x}S_{14}$ ($x \approx 2.6$), which was synthesized by reacting SrS/La_2S_3/Bi_2S_3 in a 1:1:1.5 ratio also at 950 °C. Again, when a smaller amount of La_2S_3 was used, $SrBi_2S_4$[27] was found in a mixture with **II**. $Cs_2La_xBi_{10-x}S_{16}$ ($x \approx 1.2$) was synthesized by reacting Cs_2S/La_2S_3/Bi_2S_3 in a 1:1:4 ratio at 900 °C. When the amount of Bi_2S_3 was increased, the main product was $CsBi_3S_5$[28] with **III** as a minor phase. For all three compounds there is a narrow range of x under which they can be obtained in pure form. The DTA and the X-ray powder diffraction results after DTA indicate that all compounds melt congruently between 740 and 860 °C; that is, **I** melts at ∼800 °C, **II** at ∼850 °C, and **III** at ∼746 °C. All compounds are semiconductors with well-defined gaps of ∼1 eV (see Figure 1). These values are very similar to those of $ALn_{1\pm x}Bi_{4\pm x}S_8$ (A = K, Rb; Ln = La, Ce, Pr, Nd) and $BaLaBi_2S_6$.

Table 4. Atomic Coordinates and Equivalent Isotropic Displacement Parameters (Å$^2 \times 10^3$) for $Cs_2La_xBi_{10-x}S_{16}$[a]

	x	y	z	U(eq)	occ
Bi(1)	0.2309(1)	0.2500	0.2582(1)	15(1)	1
Bi(2)	0.2433(1)	−0.7500	−0.0936(1)	18(1)	1
Bi(3)	0.1311(1)	−0.7500	0.3543(1)	18(1)	1
Bi(4)	0.3456(1)	−0.7500	0.0143(1)	20(1)	1
Bi(5)	0.0513(1)	−0.7500	−0.4981(1)	19(1)	1
Bi(6)	0.0472(1)	−0.7500	−0.1366(1)	17(1)	1
Bi(7)	0.0452(1)	−0.7500	0.0607(1)	17(1)	1
Bi(8)	0.1384(1)	−0.2500	−0.0456(1)	39(1)	0.632(12)
La(8)	0.1384(1)	−0.2500	−0.0456(1)	39(1)	0.368(12)
Bi(9)	0.2472(1)	−0.2500	0.0870(1)	41(1)	0.685(13)
La(9)	0.2472(1)	−0.2500	0.0870(1)	41(1)	0.315(13)
Bi(10)	0.1228(1)	−0.2500	0.1788(1)	37(1)	0.498(12)
La(10)	0.1228(1)	−0.2500	0.1788(1)	37(1)	0.502(12)
Cs(1)	−0.0115(1)	−0.7500	−0.3063(1)	21(1)	1
Cs(2)	0.3598(1)	0.2500	0.2288(1)	38(1)	1
S(1)	0.2726(2)	−0.2500	0.2163(3)	14(1)	
S(2)	0.1926(2)	0.2500	0.1568(3)	15(1)	
S(3)	0.1998(2)	−0.2500	−0.1377(3)	16(2)	
S(4)	0.1729(2)	−0.2500	0.2993(3)	22(2)	
S(5)	0.2029(2)	−0.7500	0.0035(3)	18(2)	
S(6)	0.2942(2)	−0.2500	−0.0369(4)	27(2)	
S(7)	0.0896(2)	−0.7500	0.2548(3)	16(1)	
S(8)	0.2984(2)	−0.7500	0.1065(3)	18(2)	
S(9)	0.1158(2)	−0.7500	−0.4242(3)	20(2)	
S(10)	0.0860(2)	−0.2500	−0.5839(3)	22(2)	
S(11)	−0.0217(2)	−0.7500	−0.5700(3)	16(1)	
S(12)	0.0483(2)	−0.2500	−0.2171(3)	17(1)	
S(13)	0.1225(2)	−0.7500	−0.1282(3)	16(1)	
S(14)	0.0435(2)	−0.2500	0.1470(3)	19(2)	
S(15)	0.0543(2)	−0.2500	−0.0341(3)	17(1)	
S(16)	0.1177(2)	−0.7500	0.0706(3)	16(2)	

[a] U(eq) is defined as one-third of the trace of the orthogonalized U_{ij} tensor. The number next to the metal atoms indicates the sites they belong in; e.g., La(8) and Bi(8) belong to the same cation site.

Structure Description. 1. $Pb_2La_xBi_{8-x}S_{14}$ ($x \approx 2.1$) (I). Although this structure has a dense, complicated three-dimensional framework, it can be well understood if it is separated into two substructures, one consisting of a porous framework with parallel tunnels and one consisting of infinitely long rods filling those tunnels. The porous substructure consists of thin infinite walls running diagonally along the *ac* plane in two different directions (see Figures 2 and 3a). The walls consist of distorted NaCl-type fragments that are two metal atoms thick. The angle defined by the walls is ∼70°. At the intersection point the walls form infinite Gd_2S_3-type rods. This arrangement creates tunnels with rhombus-like cross sections that are filled with infinite Bi_2Te_3-type rods. In Figure 3a some of these rods have been removed to show the tunnels. The similar sizes[29] of Pb^{2+}, Bi^{3+}, and La^{3+} result in an extensive occupancy disorder in the structure. The Pb^{2+} and Bi^{3+} disorder is very common in the lead bismuth sulfosalts,[17] while the Bi^{3+} and La^{3+} disorder is also found in $ALn_{1\pm x}Bi_{4\pm x}S_8$[23] (A = K, Rb; Ln = La, Ce, Pr, Nd).

The unit cell has 10 metal atom positions, and several of them, as mentioned earlier, display mixed occupancy. Four of these metal positions contain no La atoms at all, while the remaining six contain a significant fraction.

The La-free sites, Bi(1), Bi(2), Bi(3), and Bi(4),[30] are octahedral, having three shorter Bi−S bonds trans to three longer bonds; e.g., Bi(2) has one bond at 2.650(5) Å, two bonds at

(27) Aurivillius, B. *Acta Chem. Scand., Ser. A* **1983**, *37*, 399−407.
(28) Kanisheva, A. S.; Mikhailov, Y. N.; Lazarev, B. V.; Trippel, A. F. *Dokl. Akad. Nauk SSSR* **1980**, *252*, 96−99.
(29) Shannon, R. D. *Acta Crystallogr., Sect. A* **1976**, *32*, 751−767.

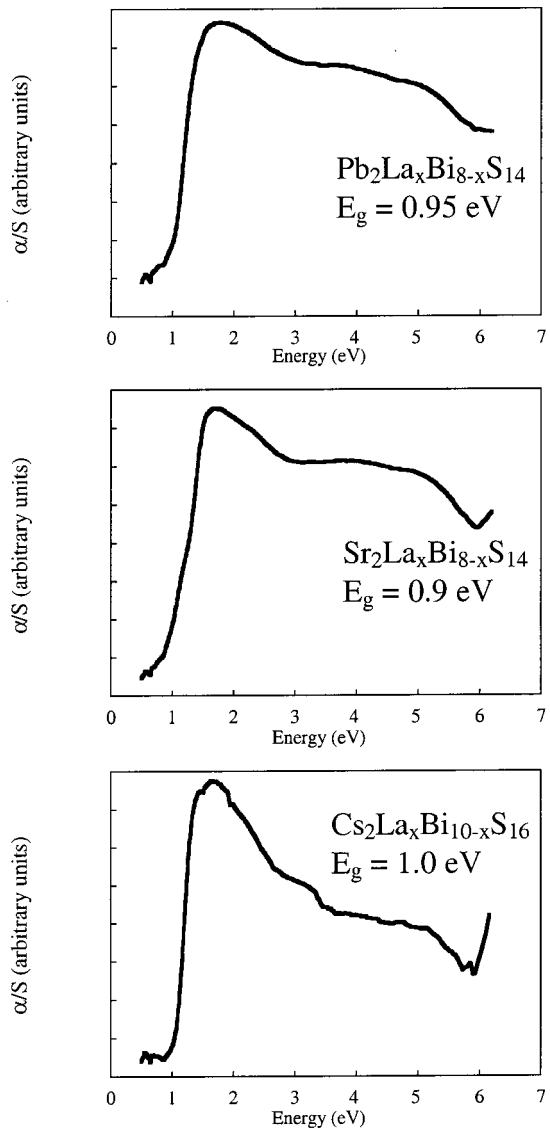

Figure 1. Solid-state UV/vis absorption spectra showing band gap transitions for $Pb_2La_xBi_{8-x}S_{14}$, $Sr_2La_xBi_{8-x}S_{14}$, and $Cs_2La_xBi_{10-x}S_{16}$.

2.674(3) Å, two bonds at 2.988(4) Å, and one bond at 2.998(5) Å. Bi(1) and Bi(2) belong to the Bi_2Te_3-type rod fragment, while Bi(3) and Bi(4) belong to the NaCl-type framework walls (see Figure 2).

The Gd_2S_3-type fragment is made up of sites M(5)/La(5) and M(6)/La(6) (see Figure 4a). The M(5)/La(5) site is seven-coordinate with monocapped trigonal coordination and distances varying between 2.795(5) and 3.029(5) Å, while site M(6)/La(6) is eight-coordinate having a bicapped trigonal prismatic coordination with distances varying between 2.875(3) and 3.248(5) Å. This fragment is also observed in $ALn_{1\pm x}Bi_{4\pm x}S_8$[23] (A = K, Rb; Ln = La, Ce, Pr, Nd), Gd_2S_3,[31] $CeTmS_3$,[32] $La_{10}Er_9S_{27}$,[33] $PbBi_2S_4$,[17a] $Pb_4In_3Bi_7S_{18}$,[34] and $La_4Bi_2S_9$.[20] One characteristic of this fragment is that the monocapped prisms form an infinite column by sharing edges while the bicapped prisms stack by sharing trigonal faces. This arrangement causes the two different kinds of prism to be disposed perpendicular to each other.

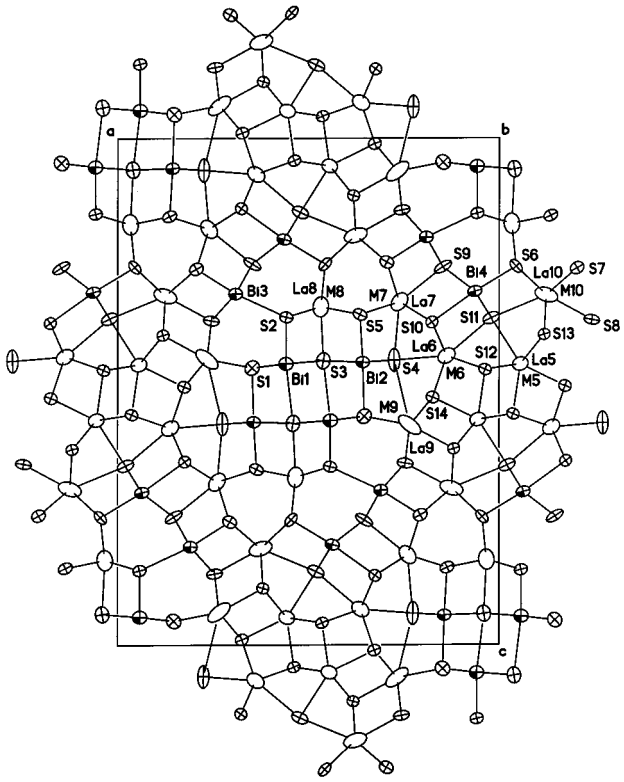

Figure 2. Projection of the structure of $Pb_2La_xBi_{8-x}S_{14}$ down the *b* axis (ORTEP view). The shaded crossed ellipsoids represent Bi atoms, the crossed ellipsoids represent S atoms, and the plain ellipsoids represent the mixed occupancy sites.

The infinite Bi_2Te_3-type rod fragment is made up of two octahedral sites Bi(1) and Bi(2) and site M(8)/La(8), which is seven-coordinate, with M(8)/La(8)−S distances varying between 2.852(3) and 3.134(4) Å (see Figure 2).

The NaCl-type walls are made up of octahedral sites Bi(3) and Bi(4) and the sites M(7)/La(7), M(9)/La(9), and M(10)/La(10), which have higher (>6) coordination numbers. Site M(7)/La(7) is eight-coordinate having bicapped trigonal prismatic coordination with M(7)/La(7)−S distances varying between 2.941(3) and 3.254(6) Å. Site M(9)/La(9) is seven-coordinate having monocapped trigonal prismatic coordination with M(9)/La(9)−S distances varying between 2.786(5) and 3.276(4) Å, while M(10)/La(10) is eight-coordinate having a bicapped trigonal prismatic coordination with M(10)/La(10)−S distances between 2.929(5) and 3.341(5) Å. Bond distances and selected angles are shown in Table 5.

As can be seen in Figure 2 the high (>6) coordinate disordered sites have at least one large anisotropic temperature factor. This feature is derived from the mixed occupancy in these sites. The resolution of the diffraction data was not sufficient to allow the modeling of these sites as split positions, although this was possible in the case of **II** (see below).

(30) (a) We believe that the octahedral sites 1−4 are occupied almost exclusively by Bi atoms. This is supported by the structure of the Sr analogue where there is no doubt for the identity of these sites. Also bond-valence calculations in $Pb_2La_xBi_{8-x}S_{14}$ indicate that these four octahedral sites should be occupied by Bi. For the remaining six sites, which contain La, the bond-valence results are harder to evaluate because there is always the possibility of a triple Pb/La/Bi disorder. Bond-valence sums in $Pb_2La_xBi_{8-x}S_{14}$ are 2.897 for Bi(1), 3.117 for Bi(2), 3.050 for Bi(3), and 3.048 for Bi(4) ($R_0 = 2.552$, $B = 0.370$). By use of the same parameters, the bond-valence sums in $Sr_2La_xBi_{8-x}S_{14}$ are 2.976 for Bi(1), 3.193 for Bi(2), 3.076 for Bi(3), and 3.072 for Bi(4). (b) VALENCE, version 2.00, distributed by I. D. Brown, Institute for Materials Research, McMaster University, Hamilton, Ontario, L8S 4M1, Canada.

(31) Prewitt, C. T.; Sleight, A. W. *Inorg. Chem.* **1968**, *7*, 1090−1093.
(32) Rodier, N. *Bull. Soc. Fr. Mineral. Cristallogr.* **1973**, *96*, 350−355.
(33) Carre, D.; Laruelle, P. *Acta Crystallogr., Sect. B* **1973**, *29*, 70−73.
(34) Krämer, V.; Reis, I. *Acta Crystallogr., Sect. C* **1986**, *42*, 249−251.

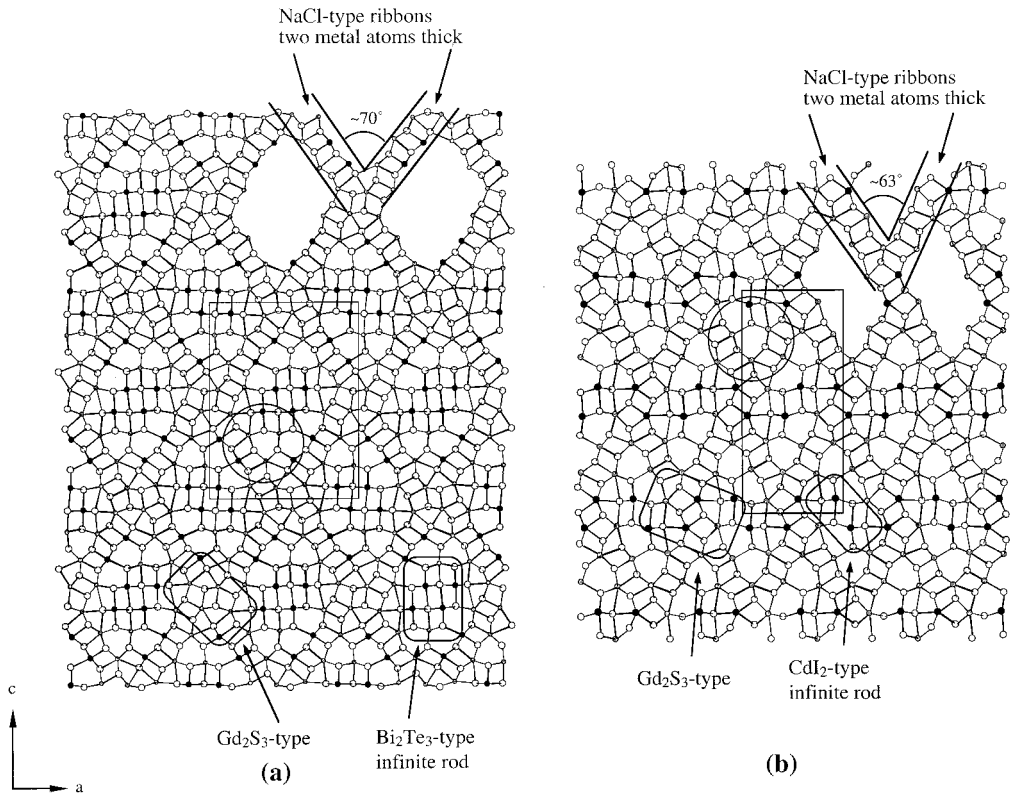

Figure 3. Comparison of two related structures: (a) projection of the structure $Pb_2La_xBi_{8-x}S_{14}$ down the *b* axis, where the black circles are Bi atoms, the white circles are the S atoms, and the gray circles represent the mixed occupancy sites; (b) projection of the structure $La_4Bi_2S_9$ down the *b* axis, where the black circles are Bi atoms, the white circles are the S atoms, and the gray circles represent the La sites. The shaded rectangular areas indicate the Bi_2Te_3- and Gd_2S_3-type building blocks. The arrows indicate the direction of the NaCl-type walls, whereas the shaded circular area shows the triangular fragment made of three trigonal prismatic sites. The same walls exist in both structures, but $La_4Bi_2S_9$ contains only a CdI_2-type fragment in the space formed between the ribbons. For clarity reasons some of the Bi_2Te_3- and CdI_2-type have been removed to show the framework walls and rhombus-like tunnels.

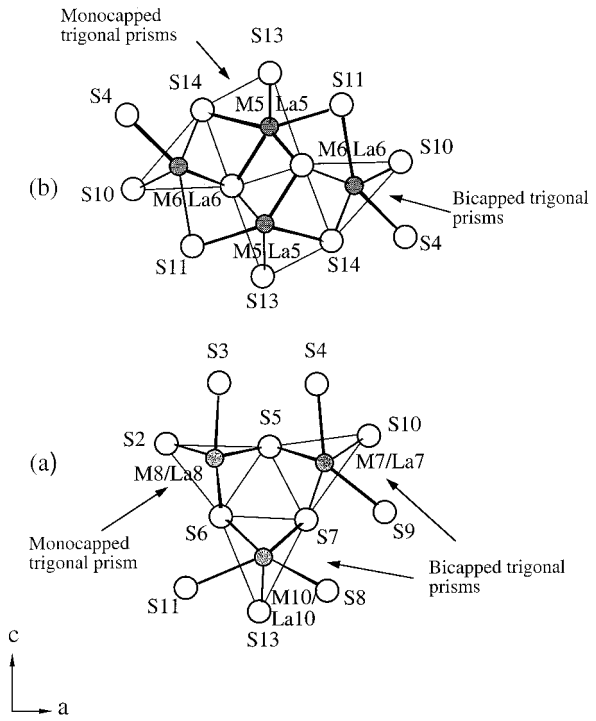

Figure 4. Projection of the triangular fragment (a) made of three trigonal prismatic sites and the Gd_2S_3-type (b) building blocks in $Pb_2La_xBi_{8-x}S_{14}$ down the *b* axis. The different kinds of trigonal prisms are also shown.

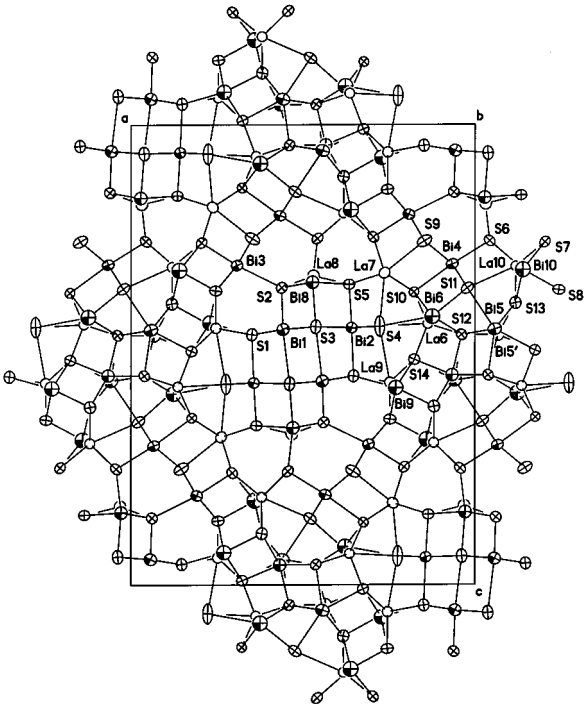

Figure 5. Projection of the structure of $Sr_2La_xBi_{8-x}S_{14}$ down the *b* axis (ORTEP view). Because of the better quality diffraction data, the splitting of the high coordinate sites can be seen. The shaded crossed ellipsoids represent Bi atoms, the crossed ellipsoids represent the S atoms, and the plain ellipsoids represent the mixed occupancy sites. For these sites, for clarity reasons, only the La atoms are shown.

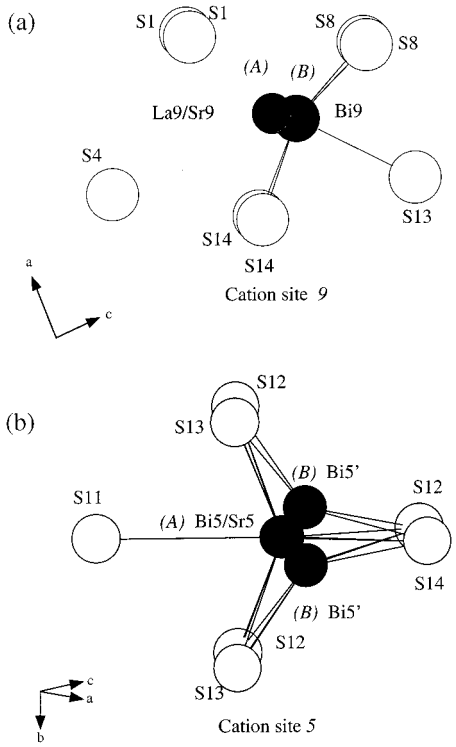

Figure 6. Coordination environments of cation site 9 (a) and cation site 5 (b) in $Sr_2La_xBi_{8-x}S_{14}$. The splitting at every site is also shown. Position A refers to the position located in the center of the site, while position B refers to the site shifted away from the center to the side.

Table 5. Bond Distances (Å) and Selected Angles (deg) for $Pb_2La_xBi_{8-x}S_{14}$

Bi(1)−S(2)	2.584(5)	S(2)−Bi(1)−S(3)	86.63(12)
Bi(1)−S(1)	2.775(4) × 2	S(2)−Bi(1)−S(1)	94.86(13)
Bi(1)−S(3)	2.908(4) × 2	S(2)−Bi(1)−S(3)	172.85(13)
Bi(1)−S(3)	3.323(5)		
Bi(2)−S(5)	2.650(5)	S(3)−Bi(2)−S(3)	85.10(13)
Bi(2)−S(4)	2.674(3) × 2	S(4)−Bi(2)−S(4)	98.19(16)
Bi(2)−S(3)	2.988(4) × 2	S(4)−Bi(2)−S(3)	172.44(12)
Bi(2)−S(1)	2.998(5)		
Bi(3)−S(7)	2.596(5)	S(7)−Bi(3)−S(8)	83.24(12)
Bi(3)−S(9)	2.781(3) × 2	S(8)−Bi(3)−S(2)	102.01(11)
Bi(3)−S(8)	2.858(3) × 2	S(9)−Bi(3)−S(8)	170.93(15)
Bi(3)−S(2)	3.123(5)		
Bi(4)−S(11)	2.673(3) × 2	S(10)−Bi(4)−S(9)	77.75(12)
Bi(4)−S(6)	2.688(4)	S(6)−Bi(4)−S(9)	105.55(12)
Bi(4)−S(10)	2.940(5)	S(11)−Bi(4)−S(9)	163.76(14)
Bi(4)−S(9)	3.019(4) × 2		
M(5)/La(5)−S(12)	2.795(5)	M(8)/La(8)−S(2)	2.852(3) × 2
M(5)/La(5)−S(14)	2.802(5)	M(8)/La(8)−S(3)	3.007(5)
M(5)/La(5)−S(12)	2.835(3) × 2	M(8)/La(8)−S(5)	3.008(4) × 2
M(5)/La(5)−S(13)	2.923(3) × 2	M(8)/La(8)−S(6)	3.134(4) × 2
M(5)/La(5)−S(11)	3.029(5)		
M(6)/La(6)−S(10)	2.875(3) × 2	M(9)/La(9)−S(13)	2.786(5)
M(6)/La(6)−S(4)	2.922(5)	M(9)/La(9)−S(14)	2.836(3) × 2
M(6)/La(6)−S(12)	3.039(4) × 2	M(9)/La(9)−S(8)	2.947(3) × 2
M(6)/La(6)−S(14)	3.152(4) × 2	M(9)/La(9)−S(1)	3.276(4) × 2
M(6)/La(6)−S(11)	3.248(5)		
M(7)/La(7)−S(10)	2.941(3) × 2	M(10)/La(10)−S(8)	2.929(5)
M(7)/La(7)−S(5)	3.063(4) × 2	M(10)/La(10)−S(13)	2.988(3) × 2
M(7)/La(7)−S(7)	3.090(4) × 2	M(10)/La(10)−S(7)	3.055(4) × 2
M(7)/La(7)−S(9)	3.111(5)	M(10)/La(10)−S(6)	3.090(4) × 2
M(7)/La(7)−S(4)	3.254(6)	M(10)/La(10)−S(11)	3.341(5)

Another characteristic of the structure is the existence of small infinite rods running along the *b* axis made up of three trigonal prisms. Along the *b* axis the trigonal prisms stack on top of each other, sharing trigonal faces, while they share edges in the *ac* plane (see Figures 3a and 4b). These rods are made up of two bicapped trigonal prismatic sites, M(7)/La(7) and M(10)/La(10), and one monocapped trigonal prismatic M(8)/La(8). The

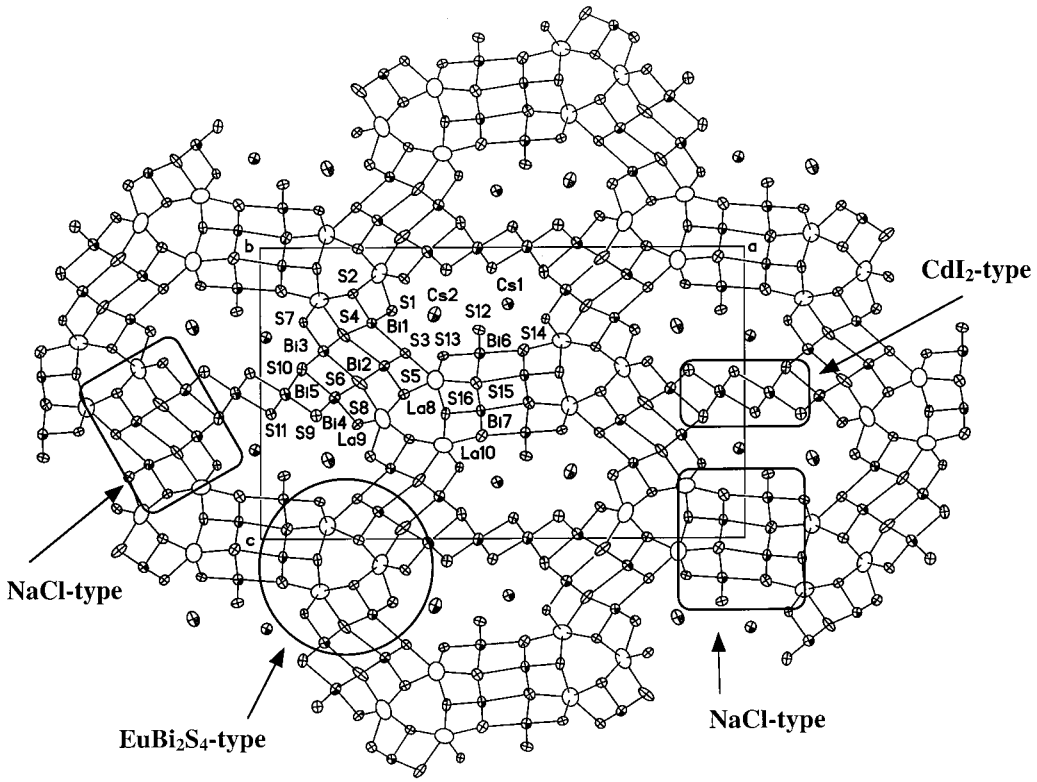

Figure 7. Projection of the structure of $Cs_2La_xBi_{10-x}S_{16}$ down the *b* axis (ORTEP view). The surrounded areas indicate the NaCl- and CdI_2-type building blocks. The circular area shows the $EuBi_2S_4$-type fragment made of three bicapped trigonal prismatic sites.

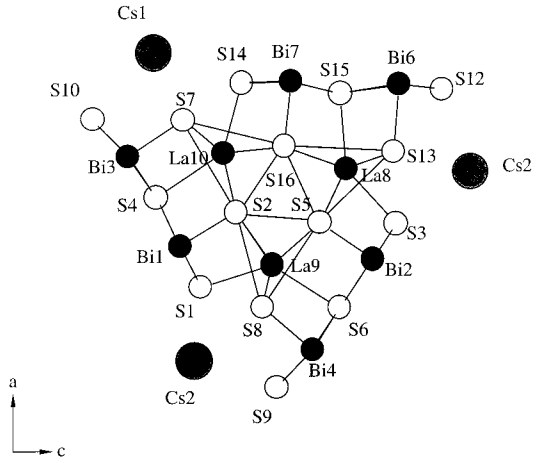

Figure 8. Projection of the $EuBi_2S_4$-type fragment found in $Cs_2La_xBi_{10-x}S_{16}$ down the *b* axis. The fragment has pseudo-C_3 symmetry and is made up of three bicapped trigonal prismatic sites (La8, La9, and La10) that display mixed La/Bi occupancy.

same motif is also found in $Cs_2La_{1+x}Bi_{9-x}S_{16}$ with the only difference being that the three sites are bicapped trigonal prismatic and the whole fragment exhibits almost 3-fold local symmetry (see below).

$Pb_2La_xBi_{8-x}S_{14}$ shares some structure features with $La_4Bi_2S_9$ [20] (see Figure 3). Both structures have the NaCl-type walls running along the *ac* plane, forming Gd_2S_3-type fragments at the point where they intersect. In the case of $La_4Bi_2S_9$ the rhombus-like tunnel that is formed between opposite running walls is significantly narrower and contains a thinner fragment, CdI_2-type, compared to the Bi_2Te_3-type fragment found in Pb_2La_x-$Bi_{8-x}S_{14}$. Furthermore, the angle defined by the walls in La_4-Bi_2S_9 is smaller (~63°). This relationship between the two compounds is very interesting because it hints of a possible homologous series of compounds that feature porous substructures made up of NaCl-type walls forming tunnels of larger cross section.

2. $Sr_2La_xBi_{8-x}S_{14}$ ($x \approx 2.6$). This compound adopts the same structure as $Pb_2La_xBi_{8-x}S_{14}$. It is not unusual for the Sr and Pb analogues to adopt the same structure given their similar size.[29] The quality of the diffraction data of **II** enabled us to better resolve the splitting of the five metal sites (see Figure 5). The coordination environments and distances for Bi(1) through Bi(4) are very similar in the two compounds; e.g., for Bi(4) the Bi−S distances in **II** vary between 2.669(2) and 3.003(2) Å, while for the same atom in **I** the distances vary between 2.673(3) and 3.019(4) Å. Also, for site 7, which does not exhibit a splitting, the distances are very similar; e.g., in **I** the M(7)/La(7)−S distances vary between 2.941(3) and 3.254(6) Å, while in **II** the La(7)/Sr(7)−S distances vary between 2.957(2) and 3.278(3) Å. The difference in distances is greater in the sites that exhibit splitting in **II**. For example, site 9 in $Pb_2La_{2+x}Bi_{6-x}S_{14}$ has distances between 2.786(5) and 3.276(4) Å while in **II** site 9 contains two positions, one square pyramidal occupied by Bi with Bi(9)−S distances between 2.618(3) and 2.895(2) Å, and the other bicapped trigonal prismatic occupied by La and Sr with distances La(9)/Sr(9)−S between 2.888(2) and 3.507(4) Å (see Figure 6a). The two positions are 0.495(1) Å apart. The same situation occurs for sites 6, 8, and 10. The assignment of the atoms in these split positions was made on the basis of the bond distances.

A significant difference between the two compounds is the behavior of site 5. In **I**, the site is disordered between M(5) (Pb or Bi) and La(5), whereas in **II** for site 5, we have an unusual splitting perpendicular to the *ac* plane. As seen in Figure 6b, Bi(5)/Sr(5) is sitting on the mirror plane with distances between 2.821(3) and 3.037(2) Å while Bi(5′) is shifted up and below the mirror plane toward the faces of the trigonal prism having four short distances between 2.559(9) and 2.710(8) Å and three long ones between 3.34(1) and 3.45(1) Å. This is an unusual coordination for Bi; yet both positions had to be assigned mainly as Bi because they were refined freely to a total occupancy of 98%. The introduction of Sr in site 5 was made for electroneutrality reasons (see structure solution section). Site 5 together with site 6 belongs to the Gd_2S_3-type fragment. This splitting is a real structural feature of **II** because all four data sets that we collected exhibited the same exact characteristics. There

Table 6. Bond Distances (Å) and Selected Angles (deg) for $Sr_2La_xBi_{8-x}S_{14}$

Bi(1)−S(2)	2.553(2)	S(2)−Bi(1)−S(3)	88.08(6)
Bi(1)−S(1)	2.808(2) × 2	S(2)−Bi(1)−S(1)	95.04(6)
Bi(1)−S(3)	2.860(2) × 2	S(2)−Bi(1)−S(3)	174.94(7)
Bi(1)−S(3)	3.368(3)		
Bi(2)−S(5)	2.650(2)	S(3)−Bi(2)−S(3)	84.73(6)
Bi(2)−S(4)	2.656(2) × 2	S(4)−Bi(2)−S(4)	99.07(9)
Bi(2)−S(1)	2.971(3)	S(4)−Bi(2)−S(3)	172.25(6)
Bi(2)−S(3)	2.999(2) × 2		
Bi(3)−S(7)	2.594(2)	S(7)−Bi(3)−S(8)	84.47(6)
Bi(3)−S(9)	2.779(2) × 2	S(8)−Bi(3)−S(2)	99.94(6)
Bi(3)−S(8)	2.862(2) × 2	S(9)−Bi(3)−S(8)	172.60(8)
Bi(3)−S(2)	3.082(2)		
Bi(4)−S(11)	2.669(2) × 2	S(10)−Bi(4)−S(9)	79.57(6)
Bi(4)−S(6)	2.715(2)	S(6)−Bi(4)−S(9)	103.58(6)
Bi(4)−S(10)	2.907(2)	S(11)−Bi(4)−S(9)	165.79(7)
Bi(4)−S(9)	3.003(2) × 2		
Bi(5)/Sr(5)−S(14)	2.821(3)	Bi(5′)-S(14)	2.559(9)
Bi(5)/Sr(5)−S(12)	2.849(2)	Bi(5′)-S(12)	2.590(8)
Bi(5)/Sr(5)−S(13)	2.881(2) × 2	Bi(5′)-S(12)	2.710(8) × 2
Bi(5)/Sr(5)−S(12)	2.895(2) × 2	Bi(5′)-S(12)	3.344(12)
Bi(5)/Sr(5)−S(11)	3.037(2)	Bi(5′)-S(13)	3.351(12)
Bi(5)/Sr(5)−Bi(5′)	0.61(1)	Bi(5′)-S(11)	3.453(12)
Bi(5′)-Bi(5′)	0.95(2)		
Bi(5′)-Bi(5′)	3.09(2)	Bi(5′)−Bi(5)/ Sr(5)−Bi(5′)	101.9(14)
La(6)/Sr(6)−Bi(6)	0.51(3)		
La(6)/Sr(6)−S(10)	2.925(2) × 2	Bi(6)−S(10)	2.75(1) × 2
La(6)/Sr(6)−S(4)	2.967(3)	Bi(6)−S(11)	2.76(3)
La(6)/Sr(6)−S(12)	2.971(2) × 2	Bi(6)−S(12)	2.93(1) × 2
La(6)/Sr(6)−S(14)	3.098(2) × 2	Bi(6)−S(4)	3.28(2)
La(6)/Sr(6)−S(11)	3.249(3)	Bi(6)−S(14)	3.50(2) × 2
La(7)/Sr(7)−S(10)	2.957(2) × 2		
La(7)/Sr(7)−S(5)	3.051(2) × 2		
La(7)/Sr(7)−S(7)	3.071(2) × 2		
La(7)/Sr(7)−S(9)	3.135(3)		
La(7)/Sr(7)−S(4)	3.278(3)		
La(8)/Sr(8)−Bi(8)	0.386(7)		
La(8)/Sr(8)−S(2)	2.903(2) × 2	Bi(8)−S(3)	2.728(9)
La(8)/Sr(8)−S(5)	3.031(2) × 2	Bi(8)−S(2)	2.793(3) × 2
La(8)/Sr(8)−S(6)	3.070(3) × 2	Bi(8)−S(5)	3.034(3) × 2
La(8)/Sr(8)−S(3)	3.105(4)	Bi(8)−S(6)	3.370(7) × 2
La(9)/Sr(9)−Bi(9)	0.495(1)		
La(9)/Sr(9)−S(14)	2.888(2) × 2	Bi(9)−S(13)	2.618(3)
La(9)/Sr(9)−S(1)	3.033(2) × 2	Bi(9)−S(8)	2.834(2) × 2
La(9)/Sr(9)−S(8)	3.046(2) × 2	Bi(9)−S(14)	2.895(2) × 2
La(9)/Sr(9)−S(13)	3.100(3)	Bi(9)−S(1)	3.371(3) × 2
La(9)/Sr(9)−S(4)	3.507(4)		
La(10)/Sr(10)−Bi(10)	0.49(1)		
La(10)/Sr(10)−S(13)	3.015(2) × 2	Bi(10)−S(8)	2.57(1)
La(10)/Sr(10)−S(6)	3.035(2) × 2	Bi(10)−S(13)	2.901(5) × 2
La(10)/Sr(10)−S(8)	3.055(3)	Bi(10)−S(7)	2.977(5) × 2
La(10)/Sr(10)−S(7)	3.100(2) × 2	Bi(10)−S(6)	3.39(1) × 2
La(10)/Sr(10)−S(11)	3.276(3)	Bi(10)−S(11)	3.61(1)

Table 7. Bond Distances (Å) and Selected Angles (deg) for $Cs_2La_xBi_{10-x}S_{16}$

Bi(1)−S(2)	2.556(6)	S(1)−Bi(1)−S(3)	80.11(15)
Bi(1)−S(1)	2.659(4) × 2	S(4)−Bi(1)−S(3)	107.10(15)
Bi(1)−S(4)	3.002(5) × 2	S(2)−Bi(1)−S(3)	164.30(18)
Bi(1)−S(3)	3.295(6)		
Bi(2)−S(5)	2.520(6)	S(6)−Bi(2)−S(4)	77.59(17)
Bi(2)−S(3)	2.710(4) × 2	S(3)−Bi(2)−S(4)	102.90(15)
Bi(2)−S(6)	2.962(5) × 2	S(5)−Bi(2)−S(4)	162.26(18)
Bi(2)−S(4)	3.720(7)		
Bi(3)−S(7)	2.583(6)	S(4)−Bi(3)−S(6)	83.86(16)
Bi(3)−S(4)	2.769(4) × 2	S(10)−Bi(3)−S(6)	95.62(15)
Bi(3)−S(10)	2.896(5) × 2	S(7)−Bi(3)−S(6)	166.00(18)
Bi(3)−S(6)	3.505(8)		
Bi(4)−S(8)	2.578(6)	S(8)−Bi(4)−S(6)	84.11(19)
Bi(4)−S(9)	2.775(4) × 2	S(6)−Bi(4)−S(10)	102.14(18)
Bi(4)−S(6)	2.928(5) × 2	S(9)−Bi(4)−S(6)	170.3(2)
Bi(4)−S(10)	3.187(7)		
Bi(5)−S(11)	2.712(4) × 2	S(10)−Bi(5)−S(10)	85.35(18)
Bi(5)−S(9)	2.756(7)	S(11)−Bi(5)−S(11)	97.3(2)
Bi(5)−S(11)	2.981(6)	S(11)−Bi(5)−S(10)	173.88(14)
Bi(5)−S(10)	3.002(5)2		
Bi(6)−S(13)	2.635(6)	S(13)−Bi(6)−S(15)	82.43(15)
Bi(6)−S(12)	2.673(4) × 2	S(12)−Bi(6)−S(12)	99.2(2)
Bi(6)−S(15)	3.010(5) × 2	S(12)−Bi(6)−S(15)	171.18(15)
Bi(6)−S(14)	3.173(6)		
Bi(7)−S(16)	2.541(6)	S(16)−Bi(7)−S(15)	87.13(16)
Bi(7)−S(14)	2.755(4) × 2	S(14)−Bi(7)−S(14)	95.2(2)
Bi(7)−S(15)	2.898(5) × 2	S(14)−Bi(7)−S(15)	174.26(17)
Bi(7)−S(15)	3.516(6)		
Bi(8)/La(8)−S(13)	2.758(4) × 2	Cs(1)−S(12)	3.491(5) × 2
Bi(8)/La(8)−S(3)	2.920(6)	Cs(1)−S(10)	3.510(7)
Bi(8)/La(8)−S(15)	2.946(6)	Cs(1)−S(11)	3.545(5) × 2
Bi(8)/La(8)−S(5)	3.213(5) × 2	Cs(1)−S(7)	3.577(5) × 2
Bi(8)/La(8)−S(16)	3.302(5) × 2	Cs(1)−S(14)	3.604(7)
Bi(9)/La(9)−S(8)	2.742(4) × 2	Cs(2)−S(8)	3.392(7)
Bi(9)/La(9)−S(1)	2.920(6)	Cs(2)−S(12)	3.409(7)
Bi(9)/La(9)−S(5)	3.122(5) × 2	Cs(2)−S(3)	3.547(6)
Bi(9)/La(9)−S(6)	3.128(8)	Cs(2)−S(1)	3.671(5) × 2
Bi(9)/La(9)−S(2)	3.166(5) × 2	Cs(2)−S(13)	3.739(5) × 2
		Cs(2)−S(9)	3.960(6) × 2
Bi(10)/La(10)−S(14)	2.849(6)		
Bi(10)/La(10)−S(7)	2.855(4) × 2		
Bi(10)/La(10)−S(16)	3.096(5)		
Bi(10)/La(10)−S(4)	3.128(7) × 2		
Bi(10)/La(10)−S(2)	3.209(5) × 2		

seems to be no indication of such a splitting in **I**. Bond distances and selected angles are shown in Table 6.

3. $Cs_2La_xBi_{10-x}S_{16}$ ($x \approx 1.2$). This compound consists of CdI_2-, NaCl-, and $EuBi_2S_4$[18]-type infinite blocks (see Figure 7) and is structurally related to the mineral kobellite,[35] $Pb_{12}(Cu,Fe)_2(Bi,Sb)_{14}S_{35}$. These blocks create tunnels filled with Cs atoms. There are two different NaCl-type blocks where the BiS_6 octahedra are severely distorted. The NaCl-type blocks are connected to each other with the $EuBi_2S_4$-type blocks. The $EuBi_2S_4$-type blocks consist of three bicapped trigonal prisms that share edges. The sites in these blocks display mixed Bi−La occupancy. The $EuBi_2S_4$-type fragment in $Cs_2La_xBi_{10-x}S_{16}$ is shown in Figure 8. Similar fragments are also found in $EuBi_2S_4$, $Eu_3Sb_4S_9$,[36] and kobellite.

As mentioned above, the BiS_6 octahedra have distorted coordination geometries. Bi(5), which belongs to the CdI_2 fragment, has the least distorted coordination with distances varying between 2.712(4) and 3.002(5) Å and angles between 85.4(2)° and 97.3(2)°. The BiS_6 octahedra of Bi(1), Bi(4), and Bi(6) are more distorted with distances varying between 2.556(6) and 3.295(6) Å, 2.578(6) and 3.187(7) Å, and 2.635(6) and 3.173(6) Å, respectively. The octahedral distortion in Bi(2), Bi(3), and Bi(7) can be described as square pyramidal with an extra Bi−S interaction above 3.5 Å; e.g., Bi(2) has one short bond at 2.520(6) Å, two bonds at 2.710(4) Å that are trans to longer bonds at 2.962(5) Å, and a long Bi−S interaction at 3.720(7) Å. Selected distances and angles are shown in Table 7.

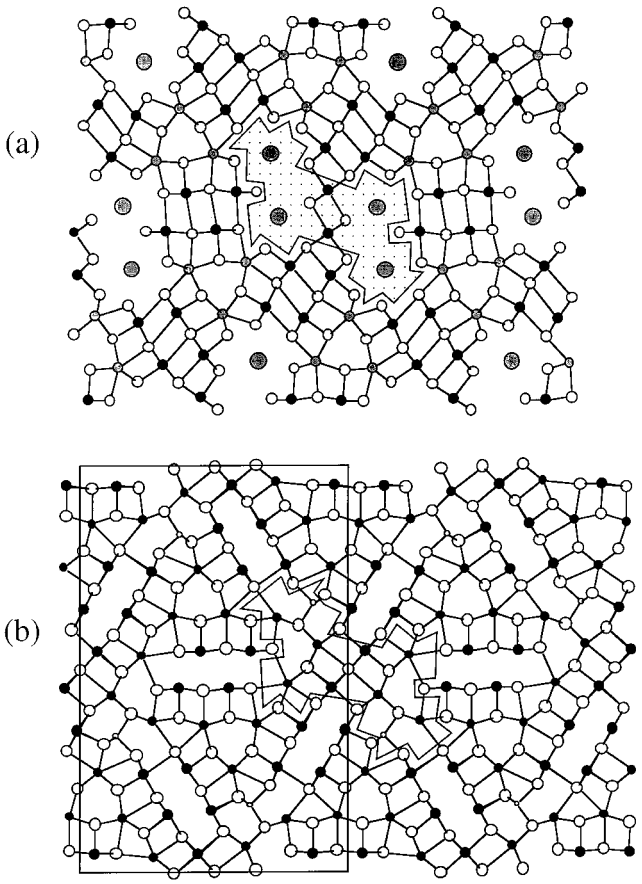

Figure 9. Comparison of the structures of (a) $Cs_2La_xBi_{10-x}S_{16}$ and (b) kobellite $Pb_{12}(Cu,Fe)_2(Bi,Sb)_{14}S_{35}$ viewed down the *b* axis. With the exception of the shaded area, the rest of the structure is common for the two compounds. The mineral kobellite contains an extra M_4S_3 block (see text) in the shaded area.

In the $EuBi_2S_4$-type block, the three sites with coordination numbers greater than 6 display mixed occupancy and form an arrangement that seems to have a local pseudo-C_3 symmetry (see Figures 7 and 8). All three sites are eight-coordinate (bicapped trigonal prisms), in contrast with what is found in **I** and **II** where we have two bicapped trigonal and one monocapped trigonal prismatic sites (see Figure 4a). It is noted that the same fragment in $EuBi_2S_4$ has true C_3 symmetry.

As mentioned above, the Cs atoms reside in tunnels formed by the NaCl-type and CdI_2-type fragments. Cs(1) has a bicapped trigonal prismatic coordination with Cs−S distances varying between 3.491(5) and 3.604(7) Å, while Cs(2) has a tricapped trigonal prismatic coordination with Cs−S distances varying between 3.392(7) and 3.960(2) Å.

The structure of **III** contains several similar building blocks with the mineral kobellite $Pb_{12}(Cu,Fe)_2(Bi,Sb)_{14}S_{35}$. This mineral crystallizes in the *Pnnm* (No. 58) space group with very similar cell parameters of $a = 22.575(3)$ Å, $b = 34.104(4)$ Å, and $c = 4.038(6)$ Å. Figure 9b shows the structure of kobellite for

(35) Miehe, G. *Nature (London), Phys. Sci.* **1971**, *231*, 133−134.
(36) Lemoine, P.; Carre, D.; Guittard, M. *Acta Crystallogr., Sect. B* **1982**, *37*, 1281−1284.

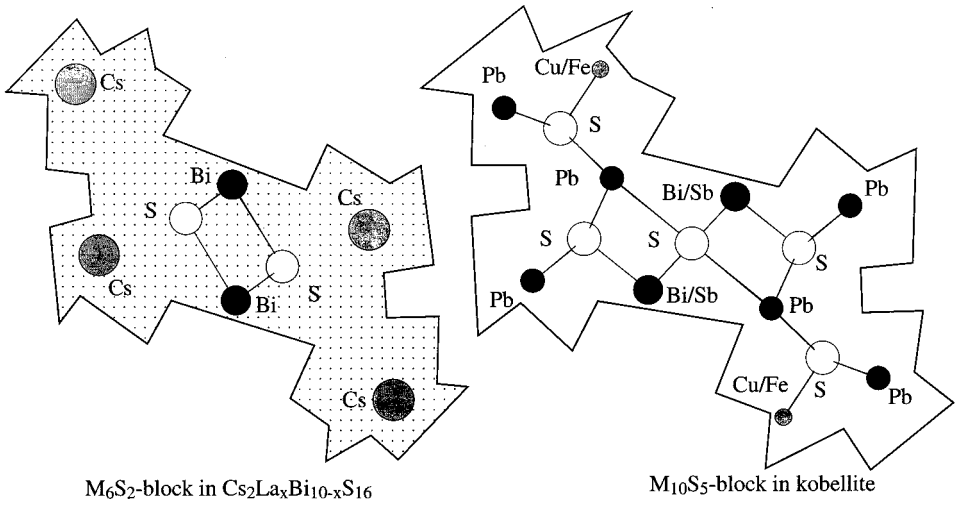

Figure 10. Comparison of the (a) M_6S_2 block in $Cs_2La_xBi_{10-x}S_{16}$ and (b) $M_{10}S_5$ in kobellite $Pb_{12}(Cu,Fe)_2(Bi,Sb)_{14}S_{35}$ viewed down the *b* axis with atom labeling.

comparison. The $EuBi_2S_4$ blocks in kobellite contain Pb atoms. A significant difference is that $Cs_2La_xBi_{10-x}S_{16}$ contains CdI_2-type fragments, whereas this is not the case for kobellite. If the formulas are compared, kobellite has the general formula $M_{28}S_{35}$ while $Cs_2La_xBi_{10-x}S_{16}$ has the general formula $M_{12}S_{16}$ or $M_{24}S_{32}$, so kobellite has an extra M_4S_3 fragment. In Figures 9 and 10, the shaded area in $Cs_2La_xBi_{10-x}S_{16}$ has four Cs atoms, two Bi atoms, and two S atoms, or a M_6S_2 block, whereas kobellite has two Cu (or Fe) atoms, six Pb atoms, two Bi (or Sb) atoms, and five sulfur atoms, or a $M_{10}S_5$ block. As a result, in the approximately same space kobellite packs an extra M_4S_3 block.

Concluding Remarks

The incorporation of La_2S_3 into the ternary bismuth chalcogenide systems A/Bi/S (A = Sr, Cs or Pb) resulted in the formation of the new compounds $Pb_2La_xBi_{8-x}S_{14}$, $Sr_2La_xBi_{8-x}S_{14}$, and $Cs_2La_xBi_{10-x}S_{16}$. The complex three-dimensional structures are new and possess building blocks that are not encountered in the simpler ternary bismuth compounds A/Bi/Q (A = alkali or alkaline earth; Q = chalcogenide) such as the Gd_2S_3-type and the $EuBi_2S_4$-type fragments described above. This leads to greater complexity, diversity, and possibilities in a system that already presents a large structural variety. For example, $La_4Bi_2S_9$ and $Pb_2La_xBi_{8-x}S_{14}$ could be regarded as the first and second members of a series of compounds that have similar framework walls but different blocks to fill the tunnels formed between the walls. A characteristic of all these systems is the extensive disorder that is encountered between the lanthanide and the bismuth atoms and sometimes the alkaline earth or Pb, and this is due to the similar size of these cations. In fact it may well be the case that the mixed occupancy is responsible for the stability of these compounds as has been determined in the case of the Nb/Ta/S, Hf/Ta/S, and Zr/Ta/Ge systems.[37]

Acknowledgment. Financial support from the Office of Naval Research (Contract N00014-98-1-0443) is gratefully acknowledged. The work made use of the SEM facilities of the Center for Advanced Microscopy at Michigan State University. The Siemens SMART platform CCD diffractometer at Michigan State University was purchased with funds from the National Science Foundation (Grant CHE-9634638).

Supporting Information Available: X-ray crystallographic files, in CIF format, for the structures **I**−**III**. This material is available free of charge via the Internet at http://pubs.acs.org.

IC001157V

(37) (a) Yao, X. Q.; Franzen, H. F. *J. Solid State Chem.* **1990**, *86*, 88−93. (b) Yao, X. Q.; Franzen, H. F. *Z. Anorg. Allg. Chem.* **1991**, *598*, 353−362. (c) Yao, X. Q.; Franzen, H. F. *J. Am. Chem. Soc.* **1991**, *113*, 1426−1427. (d) Marking, G. A.; Franzen, H. F. *J. Am. Chem. Soc.* **1993**, *115*, 6126−6130. (e) Cheng, J.; Franzen, H. F. *J. Solid State Chem.* **1996**, *121*, 362−371. (f) Richter, K. W.; Franzen, H. F. *J. Solid State Chem.* **2000**, *150*, 347−355.